Metallophysics and Advanced Technologies
Металофіз. новітні технол.
Metallofiz. Noveishie Tekhnol.
2023, vol. 45, No. 10, pp. 1151–1164
https://doi.org/10.15407/mfint.45.10.1151
Reprints available directly from the publisher

PACS numbers: 61.50.Ks, 62.20.D-, 62.50.-p, 64.30.-t, 65.60.+a, 81.40.Jj, 81.70.Bt

Equation of State and Thermal Properties of Bulk Metallic Glass under High Compressions

S. Gaurav, S. Shankar*, Arvind Mishra**, and S. P. Singh

Department of Applied Physics, Amity University,
Amity Road, Sector 125,
122413 Noida, India
**Experimental Research Laboratory, Department of Applied Physics,*
ARSD College, University of Delhi,
Dhaula Kuan Enclave I,
110021 New Delhi, India
***Department of Applied Science and Humanities,*
G. L. Bajaj Institute of Technology and Management,
201303 Noida, India

Studies on the equation of state (EOS) for solids are highly valuable in the field of condensed matter physics and geophysics. The analyses of the equation of state under high compressions for solids are already performed. In the proposed study, we have considered the four different approaches (finite strain and interionic potential) to study P–V–T relationship for amorphous glasses. The theoretically obtained results are compared with available experimental data to compare and verify the best suitable equation of state for amorphous solids like glass, which can be used in the future to find the thermodynamic parameters of bulk metallic glass, which is also an amorphous solid in total. The results obtained from Shanker EOS and higher-order Shanker EOS are found to be more consistent with the experimental results. We calculate the Grüneisen parameter and thermal conductivity for the bulk metallic glasses (window and water white glasses) under high compressions.

Key words: bulk metallic glass, equation of state, finite strain theory, Lagrangian strain, Eulerian strain, Debye temperature, thermal conductivity.

Дослідження рівнянь стану твердих тіл є важливим для фізики конденсо-

Corresponding author: Sharma Gaurav
E-mail: gsharma6@amity.edu

Citation: S. Gaurav, S. Shankar, Arvind Mishra, and S. P. Singh, Equation of State and Thermal Properties of Bulk Metallic Glass under High Compressions, *Metallofiz. Noveishie Tekhnol.*, **45**, No. 10: 1151–1164 (2023). DOI: 10.15407/mfint.45.10.1151

ваних середовищ і геофізики. Аналізу рівняння стану за високих стиснень для твердих тіл вже виконано. В даній роботі розглянуто чотири різні підходи (скінченної деформації та міжйонного потенціялу) задля дослідження P–V–T-співвідношення для аморфного скла. Теоретично одержані результати порівнюються з наявними експериментальними даними для знаходження найбільш підходящого рівняння стану для аморфних твердих речовин, яке можна використовувати для визначення термодинамічних параметрів масивного металевого скла, яке також є аморфним твердим тілом. Результати, одержані за допомогою Шенкерового рівняння та Шенкерового рівняння з врахуванням вищих порядків, виявилися найбільш узгодженими з експериментальними результатами. Було обчислено Ґрюнайзенів параметер і теплопровідність для об'ємного металевого скла (віконного та водяного білого скла) за високих тисків.

Ключові слова: масивне металеве скло, рівняння стану, теорія скінченної деформації, Лягранжева деформація, Ойлерова деформація, Дебайова температура, теплопровідність.

(Received 17 December, 2022; in final version, 12 January, 2023)

1. INTRODUCTION

Several investigations previously expressed different approaches for developing various forms of the equation of states (EOS) in order to study the behaviour of solids under high pressure [1–8]. The present investigation is an extension to the applicability and validity of existing equations of state for solids that are up to extremely high pressure, additionally, the purpose is also to search for an equation of state that is truly universal, *i.e.*, validating for both crystalline and amorphous solids. Once knowing the EOS correctly, we can use it to study the geophysical details [8–10, 20], thermoelastic properties of solids [9], and can calculate the Gibbs free energy. Nucleation of metallic glasses can be controlled and effected with powerful effects [11, 12]. Our purpose in this work is to analyse some of the important parameters of amorphous glass by applying four equations of state. The equations are derived from finite strain theory [3, 8], volume dependence of the short-range force constant derived from inters ionic potentials and pressure dependence of the bulk force constant [13, 15, 21, 22]. Bulk metallic glass possesses better properties than ordinary crystalline glass, for instance, it is twice as strong as titanium together with displaying properties of elasticity and hardness over ceramic. Due to the absence of crystallization defects, it is resistant to corrosion and wear yet can be moulded and changed even in a net. As far as the structure of bulk metallic glass (BMG) is concerned, the atoms of metallic glass are randomly frozen [23], disordered and amorphous in nature whereas the atoms of metals arrange themselves in a repeated pattern, *i.e.*, follow-

ing crystallization property. Thereafter, verifying and finding the best equation of state for amorphous solids being compatible with the experimental data, the same equation will be used to find the thermodynamic parameters for BMG.

Present work aims to assess the applicability and validity of EOS in amorphous glasses, for which the two different glasses, *i.e.*, window glass $(SiO_2)_{1-x}(Na_2O)_x$ $(x = 0.2)$, and water white glass (Na_2SiO_3) have been considered for study on the basis of availability of input data and the results are computed at high compressions using four different EOSs based on different approaches (finite strain and interionic potential). In Section 3, the results derived from these equations of state for glasses are compared with available experimental data. The behaviour of the compressibility with pressures of bulk metallic glasses is described in Sec. 4. The study based on the anharmonic behaviour and thermal conductivity for window glass and water white glass is given in Sec. 5.

2. DIFFERENT FORMS OF EQUATION OF STATE

The equation of state was derived by employing various approaches [1, 9, 11, 14]. Here, we are considering the following methods.

2.1. Equation of State Based on the Eulerian Strain

The Eulerian strain [10] is

$$\varepsilon(\eta) = \frac{1-\eta^{-2/3}}{2}\left[1-\left(\frac{V_0}{V}\right)^{-2/3}\right].$$

Using Eulerian strain, the pressure relation is

$$P(\varepsilon,0) = -3K_{T0}(1-2\varepsilon)^{-5/2}\varepsilon[1-3(K_0'-4)\varepsilon/2]. \qquad (1)$$

2.2. Equation of State Based on Lagrangian Strain

The Lagrangian strain [10] is given by

$$\varepsilon(\eta) = \frac{\eta^{2/3}-1}{2}\left[\left(\frac{V_0}{V}\right)^{2/3}-1\right].$$

The pressure expression obtained using Lagrangian strain is given by

$$P(\eta,0) = -\frac{3}{2}K_{T0}(\eta^{-1/3}-\eta^{-1/3})\left[1-\frac{3}{4}K_0'(\eta^{2/3}-1)\right]. \qquad (2)$$

2.3. B–M Third Order Equation of State

The original derivations of Birch are derived from Murnaghan's theory of finite elasticity [1, 2, 8]. Birch's EOS based on ε parameter. To the third order, the isothermal B–M equation of state is

$$P(\eta, 0) = -\frac{3}{2} K_{T0} (\eta^{-5/3} - \eta^{-7/3})[1 - 3(K_0' - 4)(1 - \eta^{-2/3}) / 4]. \quad (3)$$

2.4. Equation Based on Volume Dependence of Force Constant from Interionic Potential

Shanker EOS depicting the relationship between P and V/V_0 can also be calculated using the volume dependence. To determine volume dependence of A (force constant) [15], we take

$$A = A_0 f, \quad (4)$$

where A_0 is independent on volume and f is a function of volume or compression V/V_0.

Now, using Shanker *et al.* approach [15], the expression of P is given by

$$P = K_0 (V / V_0)^{-4/3} \left[\left(1 - \frac{1}{t} + \frac{2}{t^2} \right) (\exp(ty) - 1) + y \left(1 + y - \frac{2}{t} \right) \exp(ty) \right], \quad (5)$$

where

$$t = K_0' - \frac{8}{3}, \; y = 1 - \frac{V}{V_0}.$$

The modified form of Shanker EOS is Higher Order EOS (HOS) (taking higher order terms) is given by

$$P = K_0 (V / V_0)^{-4/3} \left[\left(1 - \frac{1}{t} + \frac{2}{t^2} - \frac{6}{t^3} \right) (\exp(ty) - 1) + \right.$$
$$\left. + y \left(1 + y - \frac{2}{t} + y^2 - \frac{3y}{t} + \frac{6}{t^2} \right) \exp(ty) \right]. \quad (6)$$

3. RESULTS AND DISCUSSIONS

Values of K_0 and K_0' used in the present calculations are shown in Table 1, which have been reported by A. K. Pandey *et al.* [16]. The results for the value of P as a function of V/V_0 down to 0.40 are given in Tables

TABLE 1. Input values of isothermal bulk modulus (K_0) and its first pressure derivative at zero pressure.

No.	Glass	K_0, GPa	K_0', GPa	γ_0
1	Window glass	38.70	2.88	1.27
2	Water white glass	45.70	1.78	0.71

TABLE 2. Variation of P *vs.* V/V_0 for window glass.

V/V_0	P, GPa (Eq. (3))	P, GPa (Eq. (5))	P, GPa (Eq. (6))	P, GPa (Eq. (2))	P, GPa (Eq. (1))	Ref. [16, 17]
1	0	0	0	0	0	0
0.9	4.727	4.742	4.744	4.68	3.33	4.74
0.8	11.686	11.863	11.885	11.22	5.55	11.86
0.7	21.87	22.802	22.935	20.16	6.66	22.8
0.6	36.374	40.146	40.673	32.25	6.63	40.15
0.5	54.841	68.943	70.609	48.70	5.44	68.95
0.4	65.885	120.2	124.928	71.57	3.11	120.21

TABLE 3. Variation of P *vs.* V/V_0 for water white glass.

V/V_0	P, GPa (Eq. (3))	P, GPa (Eq. (5))	P, GPa (Eq. (6))	P, GPa (Eq. (2))	P, GPa (Eq. (1))	Ref. [16, 17]
1	0	0	0	0	0	0
0.9	5.225	5.297	5.298	3.68	5.25	5.3
0.8	11.689	12.516	12.537	5.56	12.09	12.51
0.7	18.441	22.688	22.808	5.62	20.95	22.68
0.6	21.143	37.615	38.051	3.85	32.50	37.6
0.5	2.81	60.734	60.62	0.28	47.75	60.7
0.4	–106.841	99.418	102.713	–5.04	68.48	99.34

2, 3. It has been claimed by experimental results [16, 17].

4. VARIATION OF COMPRESSIBILITY UNDER HIGH PRESSURES

Researchers have developed a new method for controlling and influencing the nucleation and growth of metal glasses using high pressure (HP) [17, 18] causing large changes in Gibbs free energy, atomic distance and chemical bonding. For instance, molecular rearrangements can occur at high pressure, suppressing long distance nuclear diffusion in the state of super-cold liquid. Under high pressure, BMG can be crystallized into very fine-grained nanostructured materials. For

nanostructured materials derived from BMG [19], nanoparticle aggregation may be avoided by reducing frequent contamination and grain growth. Crystallization in BMG is very complex due to the primary crystallization in the super-cold liquid state and the possible phase separation before the complex diffusion flow. In addition, metal glasses respond to pressure in a complex way. In various glasses, high pressure is found to stimulate or suppress crystallization [20, 21] indicating extended scattering peaks depicting that samples (> 6 GPa) can achieve a completely amorphous phase with applied pressure using experimental techniques.

Although, when subdued at low pressure (4.5 GPa), crystalline peaks are weak but sharp and suggest a broad hump implying that a complete assessment is not possible at this pressure. However, more intense crystalline peaks superpose on broad peaks in which the volume fraction of the crystalline phases is more than 15% [24], when cooled at very low pressures (2.5 GPA).

The equation of solid state plays a vital role in applications of geophysics and condensed matter physics [11, 22, 35]. However, little is known about the EOS. As for metallic glasses, EOS measurements are primarily hampered by the inability to prepare bulk metallic glass specimens, as in the present study, we investigated the behaviour of bulk metallic glass using EOSs. It becomes possible to study various properties at high temperatures and pressures owing to the large volume and high thermal stability of the device.

In order to study the elastic wave propagation within the solid, the ultrasonic method is the governing tool and the structural and vibrational characteristics of the material can be analysed, giving important information about its sound detection capabilities. An ideal solution to studying the equation of state would be to measure the pressure-based acoustic properties. In this work, we have studied EOS for bulk metallic glasses and predicted suitability for it. We have used Eq. (1) to Eq. (3), Eq. (5), and Eq. (6), and the results are shown in Table 2. Few findings are the next.

The compressibility of solids is determined by the nature of the interatomic potential and atomic configurations, and therefore, the findings above suggest that BMG's short-distance order structure is correlated with their metal components atomic configuration (Table 2). A correlation is found between the BMG curves and their metallic components, which indicate a different average result for each element. Shankar EOS and high order Shankar EOS, derived from the atomic potential approach, are more reliable and closer to the results of experiments [16, 17, 23] shown in Tables 2 and 3.

The behaviour of bulk metallic glasses of more than 6 GPa is examined in Figs. 1, 2. At low pressures, the window glass shows a full crystalline phase but with increasing pressure it loses its crystalline phase,

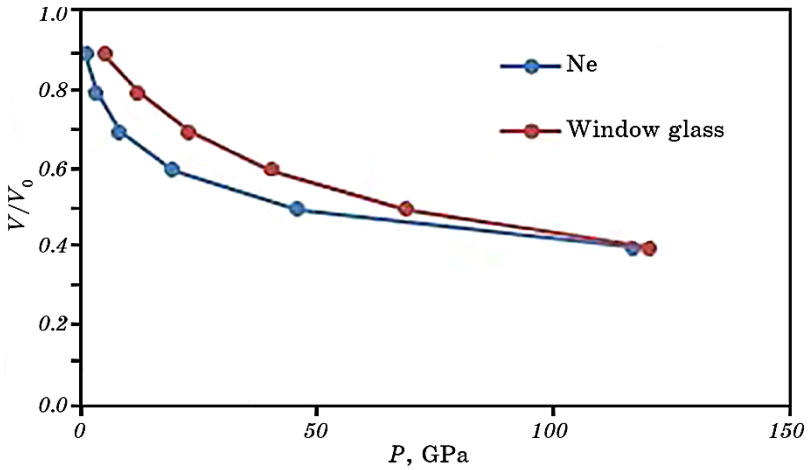

Fig. 1. Variation of *P versus* V/V_0 for window glass and Ne.

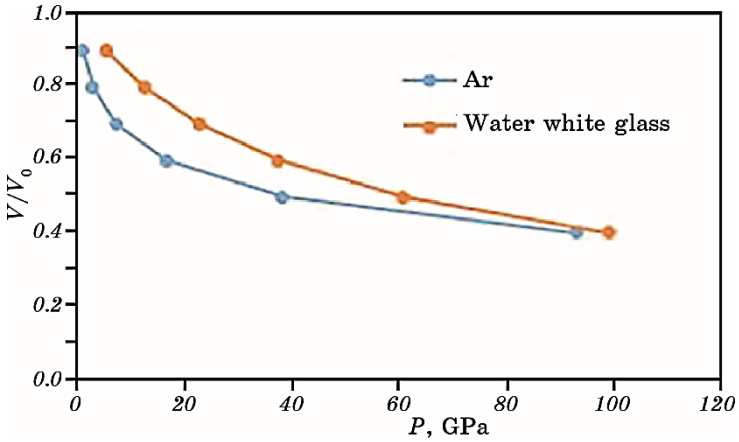

Fig. 2. Variation of *P versus* V/V_0 for water white glass and Ar.

close to Ne (at low pressures, the window glass shows a complete crystalline phase, but loses its crystalline phase with increasing pressure, close to Ne) [12, 24]. At the same time, the water white glass is similar to Ar [12, 24].

5. ANHARMONICITY AND THERMAL CONDUCTIVITY OF BMG

The ratio of γ is a vital quantity in condensed matter physics as well as Shockwaves and the field of geophysics. At high Grüneisen pressure and temperature, it is known to exhibit thermodynamic behaviour. The

anharmonicity of solids is directly linked to the Grüneisen parameter. The greater the value of γ, the greater is its anharmonic nature.

The knowledge of the Grüneisen ratio is also required to obtain the thermal EOS. In geophysics, the value of the Grüneisen ratio is used to constrain geographically.

Essential parameters like pressure as well as temperature of the metal and core [8, 25]. Shock wave measurements are also a major problem while determining the functional dependence of the material on the Grüneisen ratio on volume in physics. The outcomes of shock-wave experiments provide us uninterrupted data on the compressive and thermal behaviour of metals, rocks, minerals and ceramics at high pressures and temperature. Unfortunately, data points are often rarely deployed and distributed randomly. Therefore, it is a challenge to have a perfect EOS for solid from their feedback of shock-wave loading. That is, their thermodynamic properties can easily be obtained by any simple difference. Thus, it is not only possible to obtain a reliable interpolation measurement but to predict the compressive and thermal properties of solids at high-pressure high-temperature throughout the field, obtained by shock-wave loading on a sound physical basis.

One way to get the perfect EOS for a solid from their response to shock-wave loading is to use a specific form of this dependence in conjunction with shock Hugoniot. That is why it is important to achieve an independent form of shock Hugoniot or isotherm. The Grüneisen ratio used in shock physics has not been done so far. Therefore, the purpose of the present work is to apply similar approaches to predict anharmonic behaviour of BMGs (window and water white glass).

The expressions of γ based on different approaches are given by Anderson [26]:

$$\gamma\rho = \gamma_0\rho_0 = \text{const}, \left(\frac{\rho_0}{\rho}\right) = \left(\frac{V}{V_0}\right), \tag{7}$$

Bennett *et al.* [27]:

$$\gamma = \gamma_0\rho_0 / \rho + (2/3)(1 - \rho_0 / \rho), \tag{8}$$

Thomson and Lauson [28]:

$$\gamma = \gamma_0\rho_0 / \rho + (2/3)(1 - \rho_0 / \rho)^2, \tag{9}$$

Srivastava and Sinha [29]:

$$\gamma = \gamma_0 \exp\left[\ln(2\gamma_0)\left\{\left(\frac{V}{V_0}\right)^{q} - 1\right\}\right], \tag{10}$$

where third-order Grüneisen ratio

$$q' = q_0 / \ln(2\gamma_0),$$

Rice [30]:

$$\frac{\gamma}{V} = \frac{\gamma_0}{V_0}\left[1 + \gamma_0\left(1 - \frac{V}{V_0}\right)\right]^{-1}. \quad (11)$$

When ambient conditions are met, all expressions predict splendid accuracy values. The $\gamma\rho = \gamma_0\rho_0 = \text{const}$ higher compression causes approximation to fail. It is equivalent to the expression proposed by Bennet *et al.* [27] and Rice [30]. Considering that there are physical assumptions involved, the author prefers Srivastava and Sinha's [29] model. Given, by using the response of solids to shock-wave loads, EOS could be derived for solids, author prefer Eq. (10) rather than Eq. (9) for the reason that it γ_∞ is used instead of q_0, which is not commonly used in shock physics. The variation of γ versus pressure using abovementioned approaches for window glass and water white glass is shown in Figs. 3 and 4.

The capacity of solids to transfer heat is one of their most basic features. The thermal conductivity coefficient χ, which is described by the macroscopic equation for the rate of heat energy flow per unit area $\boldsymbol{Q}$ normal to the gradient ∇T, $\boldsymbol{Q} = -\chi\nabla T$, is commonly used to quantify this attribute.

In order to design power-dissipating devices, it is crucial to understand and manage semiconductor thermal conductivity. Examples of such devices include power transistors, solar cells in bright sunlight, diodes, transistors, and semiconductor lasers all have a lot of internal

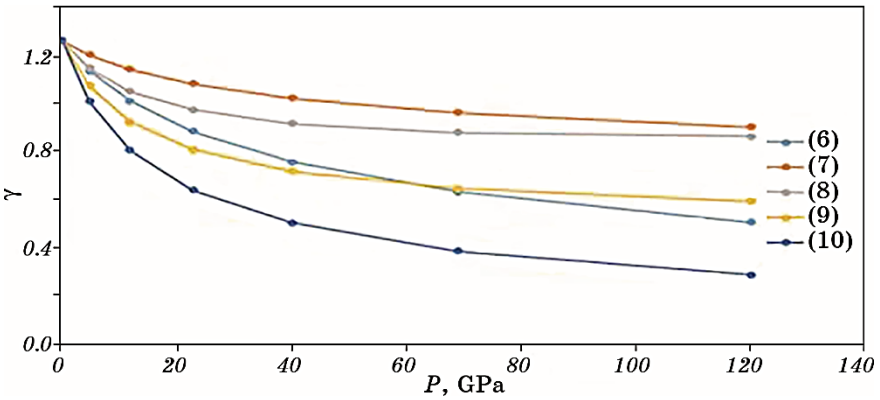

Fig. 3. Variation of γ *versus* pressure for window glass.

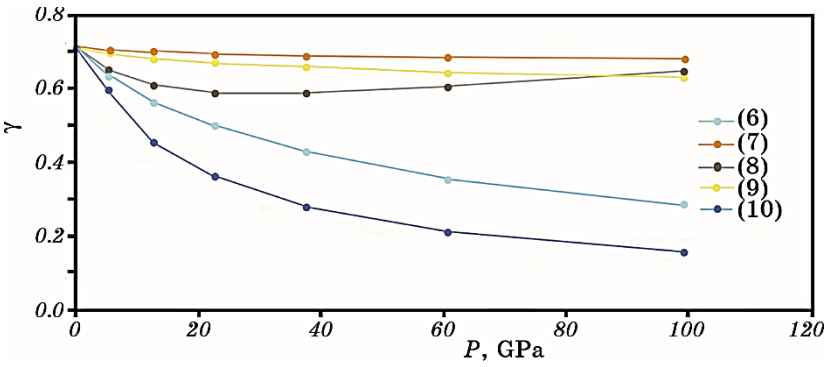

Fig. 4. Variation of γ *versus* pressure for water white glass.

power dissipation, and the device materials' high thermal conductivity can help transport that energy to a heat sink. Low heat conductivity of semiconductor alloys, on the other hand, in thermoelectric devices can be made more efficient by increasing their figure of merit.

Several types of crystalline solids are investigated for their thermal conductivity, with a focus on materials with $\kappa > 0.5$ W·cm^{-1}·K^{-1}. The lattice thermal conductivity of a solid in this domain has been examined by Slack [32] and Berman [33] using several early estimates. The values of the thermal conductivity for solids at temperatures in the vicinity of their Debye temperature can be used as approximate values for our purposes as displayed in Figs. 5 and 6.

We can now enumerate the essential parameters that make an electrically insulating substance thermally conductive using equation of Slack [32]: low n (simple crystal structure), small Grüneisen parameter, and high Debye temperature.

To determine the effects of pressure P and temperature T on thermal conductivity, we need to know how the Debye temperature parameter varies. For this, we used the following relationship:

$$\theta(P) = \theta_0 \left(1 + \frac{\gamma_0}{K_0} P\right). \tag{12}$$

Tang [34] established the following empirical relationship by using the predicted data for thermal conductivity variations with pressure:

$$\chi = A_1 + B_1 P, \tag{13}$$

where $A_1 = K_0$ and $B_1 = \chi_0/K_0(5/3 + 3\gamma_0)$, or in rewritten form:

$$\frac{\chi}{\chi_0} = \left[1 + \frac{1}{K_0}\left(\frac{5}{3} + 3\gamma_0\right) P\right]. \tag{14}$$

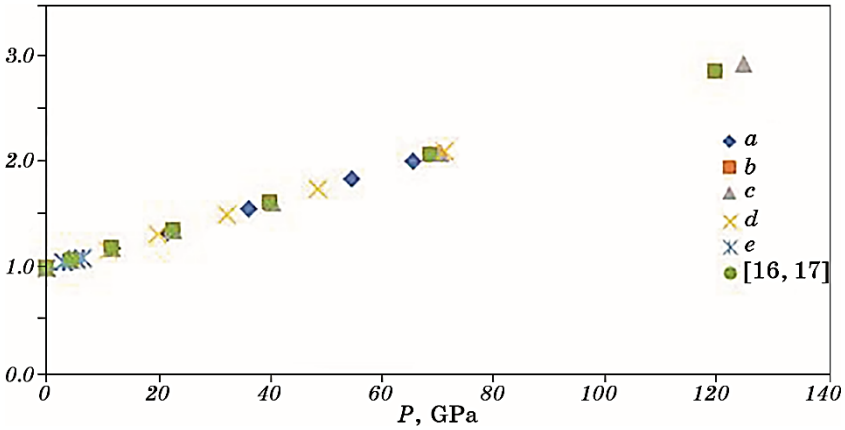

Fig. 5. Pressure dependence of Debye temperature ratio for window glass. The points predicted through the empirical relationship (12) taking pressure values from Eq. (1) (*a*), Eq. (2) (*b*), Eq. (3) (*c*), Eq. (5) (*d*), Eq. (6) (*e*) and available data [16, 17].

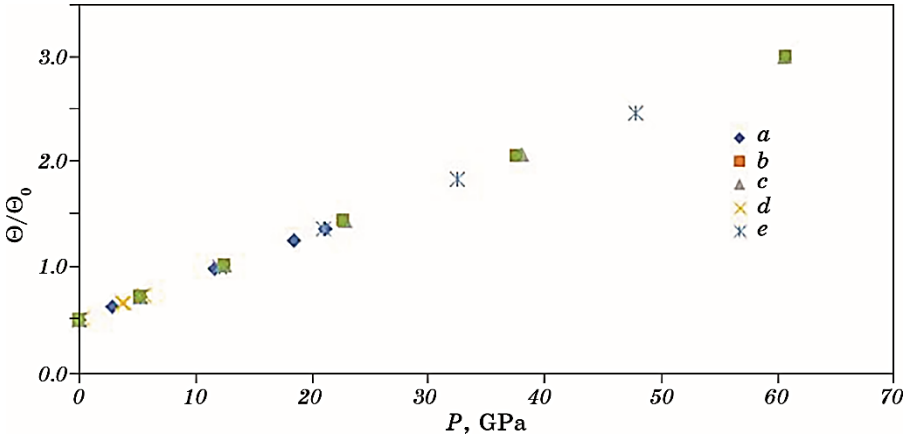

Fig. 6. Pressure dependence of Debye temperature ratio for water white glass. The points predicted through the empirical relationship (12) taking pressure values from Eq. (1) (*a*), Eq. (2) (*b*), Eq. (3) (*c*), Eq. (5) (*d*), Eq. (6) (*e*) and available data [16, 17].

The anticipated values for χ/χ_0 from Eq. (14) are shown in Figs. 7 and 8. The thermal conductivity rises with increasing pressure at constant temperature due to polar opposite type the thermal conductivity of isobaric and isothermal are changes significantly. At concurrently increased pressures and temperatures, the materials beneath consideration turn into modest due to adjustment of thermal conductivity.

Due to the lack of experimental data at high temperatures and pres-

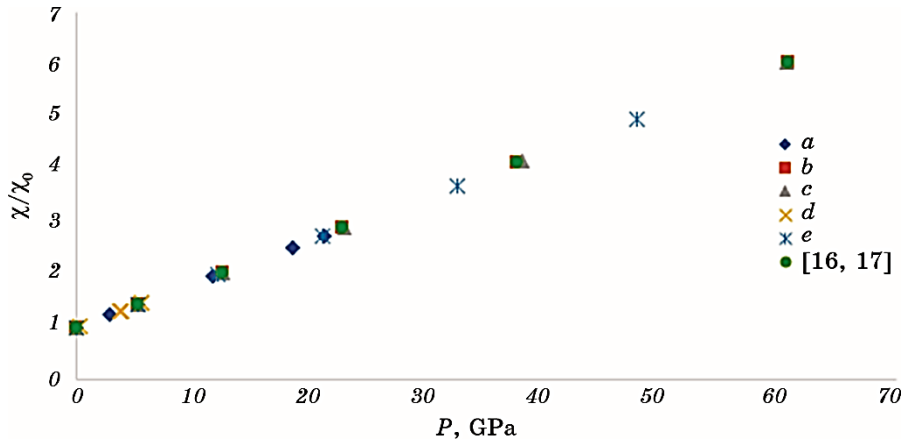

Fig. 7. Pressure dependence of thermal conductivity for water white glass at $T = 300$ K. The points predicted through the empirical relationship (13) taking pressure values from Eq. (1) (*a*), Eq. (2) (*b*), Eq. (3) (*c*), Eq. (5) (*d*), Eq. (6) (*e*) and available data [16, 17].

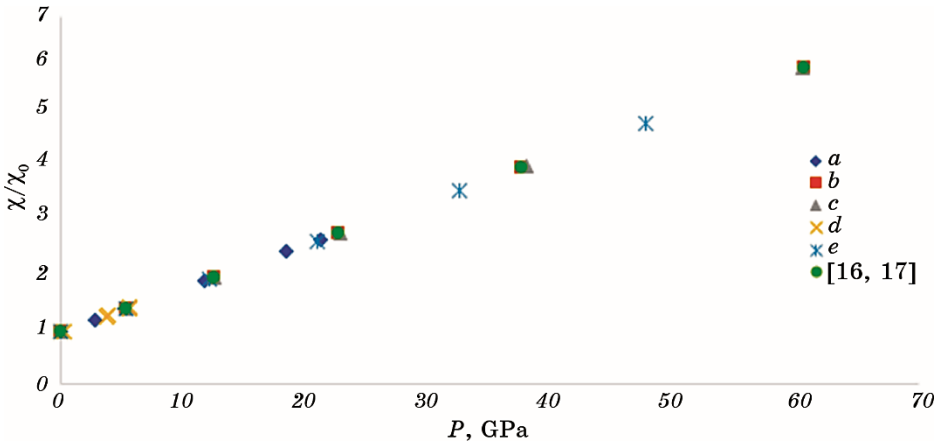

Fig. 8. Pressure dependence of thermal conductivity for window glass at $T = 300$ K. The points predicted through the empirical relationship (14) taking pressure values from Eq. (1) (*a*), Eq. (2) (*b*), Eq. (3) (*c*), Eq. (5) (*d*), Eq. (6) (*e*) and available data [16, 17].

sures, the empirical Eq. (14) is assumed to hold at these temperatures and pressures. In this work, we evaluated thermal pressure using the most trustworthy EOSs created recently by various methodologies (Eqs. (1)–(3), (5), (6), and accessible data). As a result, the data is generated by Eq. (14) and the results are achieved in this study under various pressure ranges.

Thermal conductivity, Grüneisen parameter, and Debye temperature must be connected. The analysis indicates that lower Grüneisen parameter, high Debye temperature, and high thermal conductivity closely match. Using EOS fit software [31], compute the thermal expansion values of window ($\alpha_0 = 77.91 \cdot 10^{-5}\,K^{-1}$ at 300 K) and water white glass ($\alpha_0 = 35.33 \cdot 10^{-5}\,K^{-1}$ at 300 K). Figure 8 shows a larger value of thermal expansion and a lower value of thermal conductivity of water white glass.

6. CONCLUSION

When glass materials are subjected to high compressions, P values obtained from Shanker EOS are in good agreement with those obtained from third-order B–M EOS. We have also obtained the results from higher-order Shanker EOS, which are quite relayed to the experimental results. The analysis shows the consistency of Shanker and higher-order Shanker EOS with experimental results. The present study concludes that the Shanker EOS and higher Shanker EOS are more consistent than the other EOSs and can be used to study the thermodynamic parameter and existing hardness of metallic glasses.

The window and water white glasses are predicted to be having anharmonicity. Because of the phase shift in the proximity of argon and neon gases, it will decrease at greater pressures. High-temperature and high-pressure thermal conductivity data are not accessible from experiment. The findings acquired as a result of the relation, which accurately reproduced available experimental data at low pressures.

REFERENCES

1. F. D. Stacey, B. J. Brennan, and R. D. Irvine, *Geophys. Surveys*, **4**, No. 3: 189 (1981).
2. F. Birch, *J. Geophys. Research*, **57**, No. 2: 227 (1952).
3. A. Keane, *Australian J. Phys.*, **7**, No. 2: 322 (1954).
4. C. A. Swenson, *J. Phys. Chem. Solids*, **29**, No. 8: 1337 (1968).
5. O. L. Anderson, *Equations of State of Solids for Geophysics and Ceramic Science* (Oxford: Oxford University Press: 1995).
6. D. Q. Zhao, M. X. Pan, W. H. Wang, B. C. Wei, T. Okada, and W. Utsumi, *J. Phys. Cond. Matter*, **15**, No. 50: L749 (2003).
7. W. K. Wang, H. Iwasaki, and K. Fukamichi, *J. Mater. Sci.*, **15**, No. 11: 2701 (1980).
8. F. D. Murnaghan, *Proc. National Academy of Sciences*, **30**, No. 9: 244 (1944).
9. X. Sha and R. E. Cohen, *J. Phys.: Cond. Matter*, **23**, No. 7: 075401 (2011).
10. S. S. Kushwah and J. Shanker, *Physica B: Cond. Matter*, **253**, Nos. 1–2: 90 (1998).
11. P. Vinet, J. Ferrante, J. R. Smith, and J. H. Rose, *J. Phys. C: Solid State Phys.*, **19**, No. 20: L467 (1986).

12. S. Gaurav, B. S. Sharma, S. B. Sharma, and S. C. Upadhyaya, *Physica B: Cond. Matter*, **322**, Nos. 3–4: 328 (2002).
13. B. Rao, *Bulk Metallic Glasses: Materials of Future* (2009).
14. M. Born and K. Huang, *Dynamical Theory of Crystal Lattices* (Oxford: Oxford University Press: 1954).
15. S. S. Kushwah and J. Shanker, *Physica B: Cond. Matter*, **253**, Nos. 1–2: 90 (1998).
16. A. K. Pandey, B. K. Pandey, and Rahul, *J. Alloys Comp.*, **509**, No. 11: 4191 (2011).
17. W. H. Wang, P. Wen, L. M. Wang, Y. Zhang, M. X. Pan, D. Q. Zhao, and R. J. Wang, *Appl. Phys. Lett.*, **79**, No. 24: 3947 (2001).
18. S. Zhongyi, C. Guiyu, Z. Yun, and Y. Xiujun, *Phys. Rev. B*, **39**, No. 4: 2714 (1989).
19. W. H. Wang, D. W. He, D. Q. Zhao, Y. S. Yao, and M. He, *Appl. Phys. Lett.*, **75**, No. 18: 2770 (1999).
20. W. K. Wang, H. Iwasaki, C. Suryanarayana, and T. Masumoto, *J. Mater. Sci.*, **18**, No. 12: 3765 (1983).
21. F. Ye and K. Lu, *Acta Mater.*, **47**, No. 8: 2449 (1999).
22. P. W. Bridgman, *Rev. Modern Phys.*, **18**, No. 1: 1 (1946).
23. W. H. Wang, C. Dong, and C. H. Shek, *Mater. Sci. Eng. R: Reports*, **44**, Nos. 2–3: 45 (2004).
24. J. Hama and K. Suito, *J. Phys.: Cond. Matter*, **8**, No. 1: 67 (1996).
25. F. D. Stacey, *Phys. Earth Planetary Interiors*, **89**, Nos. 3–4: 219 (1995).
26. *Thermodynamics of Deep Geophysical Media*.
27. *LA-UR-92-3407 Sesame: the Los Alamos National Laboratory Equation of State Database Contents*.
28. V. Gospodinov, *Int. J. Mod. Phys*, **28**: 1450196 (2014).
29. S. K. Srivastava and P. Sinha, *Phys. B: Cond. Matter*, **404**, No. 21: 4316 (2009).
30. M. H. Rice, *J. Phys. Chem. Solids*, **26**, No. 3: 483 (1965).
31. Ross J. Angel, Javier Gonzalez-Platas, and Matteo Alvaro, *Z. Kristallogr.*, **229**, Iss. 5: 405 (2014).
32. G. A. Slack, *Solid State Phys.*, **34**: 1 (1979); G. A. Slack, *J. Phys. Chem. Solids*, **34**, Iss. 2: 321 (1973).
33. R. Berman, *Thermal Conduction in Solids* (Oxford: Clarendon Press: 1976).
34. W. Tang, *J. Phys. Chem. Solids*, **62**, Iss. 11: 1943 (2001).
35. S. Gaurav, S. Shankar, R. Anamika, K. Pratibha, and S. Manish, *Rus. J. Earth Sci.*, **22**, No. 3: 5 (2022).